Intra- to Intermolecular Singlet Fission

Supporting Information

M. T. Trinh,[1] Y. Zhong,[1] Q. Chen,[1] T. Schiros,[1] S. Jockusch,[1] M.Y. Sfeir,[2] M. Steigerwald,[1] C. Nuckolls,[1] and X-Y. Zhu[1]

[1]Department of Chemistry, Columbia University, New York, NY 10027, USA

[2]Center for Functional Nanomaterials, Brookhaven National Laboratory, Upton, NY 11973, USA

1) Triplet sensitization experiment

Absorption spectra of $DPDC_7$ and thioxanthone (TX) in acetonitrile are shown in Fig. S1-A. Figure S1-B shows the dynamics at different wavelengths for a solution of TX (dashed curve) and a mixed solution of TX and $DPDC_7$ (solid curves). The time profile at 630 nm for TX alone (blue dashed line) shows the TX triplet decay dynamics with a time constant of 15 μs. The lifetime of the TX triplet is shortened to 5 μs (red line) in the mixed solution with $DPDC_7$, indicating triplet transfer from TX to $DPDC_7$. In this mixture, the dynamics at 520 nm (light blue) has a rise time constant of 1.8 μs; this is assigned to the buildup time for triplet in $DPDC_7$. The rise in absorption signal at 520 nm is mirrored by the bleaching signal at 440 nm (dark blue), with a similar time constant. It is important to note that the absorption of $DPDC_7$ is none zero at 355 nm (panel A) and singlets and subsequently biexciton (BE) are also generated in $DPDC_7$ upon photoexcitation. However the lifetime for singlet and biexciton in $DPDC_7$ in solution are very short, < 100 ps (main text). These singlet and BE features show up as a spike in Fig. S1B). There is no significant intersystem crossing observation in the solution of $DPDC_7$.

Figure S1-C presents the ns transient absorption spectra at different delay times. At a short time delay (0.1-0.5 μs) when the $DPDC_7$ triplet population is negligible, the absorption spectrum (blue) is mainly that for the triplet in TX. At a longer time (4-6 μs), the $DPDC_7$ triplet population dominates and absorption represents that of the T_1 state in $DPDC_7$. The T_1 absorption in $DPDC_7$ (red spectrum in Fig. S1-C) spans the range of ~500 nm to ~650 nm. Note that in the $DPDC_7$, T_1 absorption may extend further to < 500 nm, but overlaps with the bleaching makes a quantitative assessment of T_1 absorption < 500 nm difficult. For comparison, we add the induced absorption

spectrum (dashed curve) for T_1 in $DPDC_7$ thin film, as obtained from global fitting (see part 3). The T_1 spectrum from global fitting of the $DPDC_7$ thin film (black dashed) is in excellent agreement with the sensitized spectrum from $DPDC_7$ solution.

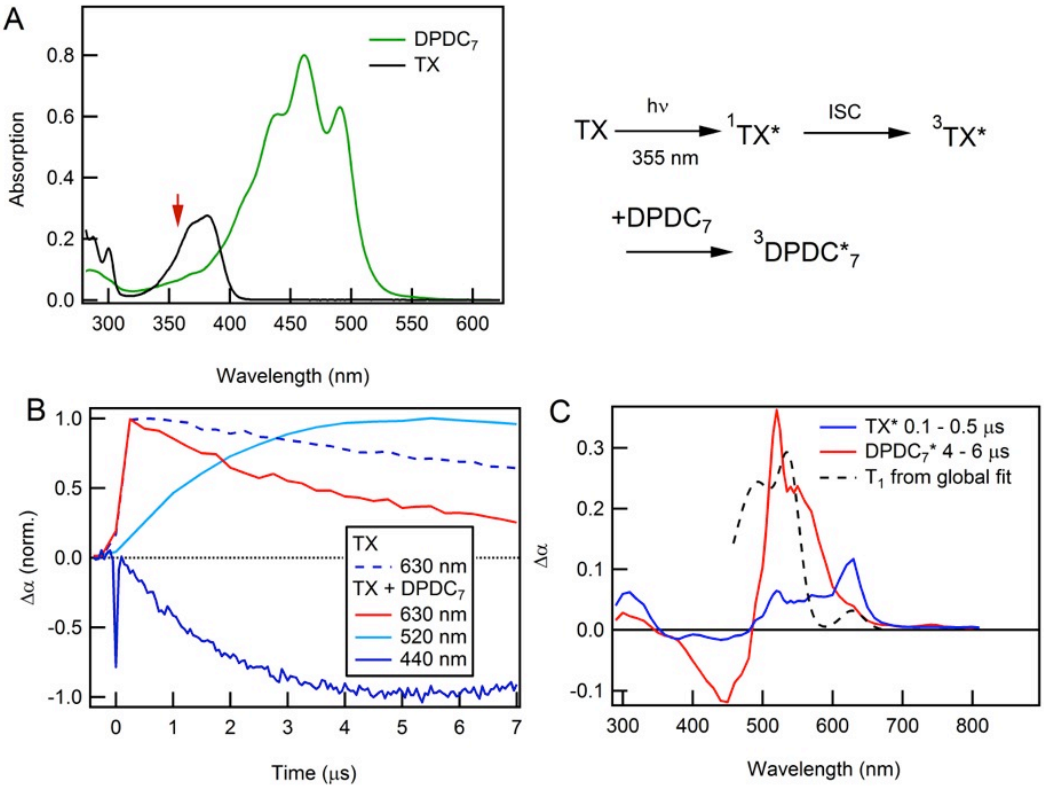

Figure S1. (**A**) Absorption spectra of $DPDC_7$ and TX in acetonitrile. The red arrow indicates the excitation wavelength for the triplet sensitization measurement. (**B**) Transient absorption dynamics for TX (dashed curve) and a mixture of TX and $DPDC_7$ (solid curves) at the indicated probe wavelengths. (**C**) Transient absorption spectra for triplet in TX (blue) and $DPDC_7$ (red). The dashed curve is the induced absorption obtained from global fit for $DPDC_7$ in solid film (Fig. 4D in main text).

2) Phosphorescence measurement

The phosphorescence spectrum from $DPDC_7$ is shown in Fig. 4B. Fig. S2 compares the phosphorescence spectrum from $DPDC_7$ to those from $DPDC_5$ and $DPDC_9$. For the phosphorescence decay dynamics in the inset in Fig. 4B, we recorded time-dependent phosphorescence decay dynamics using laser pulsed excitation (355 nm, 5 ns pulse width)

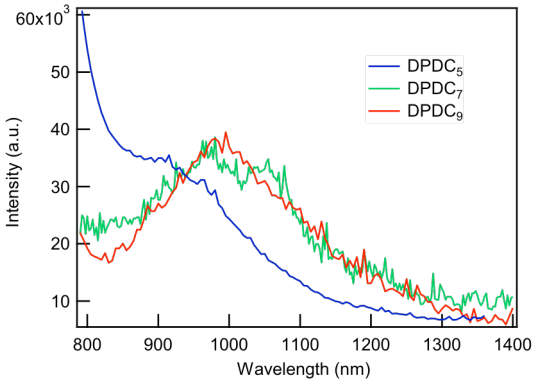

Figure S2. Phosphorescence spectrum from solids of $DPDC_{5,7,9}$ excited at 355 nm.

from a Nd:YAG laser (GCR-150-30, Spectra Physics) and a NIR sensitive PMT detector (H10330A-45, Hamamatsu).

3) Global fitting

We present global fitting based on the intra- to intermolecular singlet fission model presented in the Scheme 1 for the solid film, main text. Photo-excitation generates the lowest bright S_2 state. The S_2 exciton quickly relaxes to the dark singlet S_1 state via internal conversion process and to the biexciton (BE) state via intramolecular singlet fission.[1,2,3]. As stated in the main text, the BE is a triplet pair state that subsequently separates into two individual T_1 excitons on adjacent molecules in the solid film with a time constant of τ_{SF}. S_1 and BE can decay to S_0 with time constants of τ_{S1} and τ_{BE}, respectively.

In the global fit, we use the BE fraction, γ=[BE]/([S_1]+[BE]), as a fitting parameter. The resulting individual triplets are long lived (see Fig. 4A) and their population can be assumed to be constant on the time scale of interest. We assume the following spectral components: 1) GB of the $S_0 \rightarrow S_2$ transition; 2) excited state absorption (ESA) of the singlet S_1; and 3) ESA of the triplets. To minimize the number of variables, we do not distinguish the ESA spectra from the triplet pair on one molecule (BE) and uncorrelated triplet (2xT_1).

The induced absorption or ESA dynamics in the spectral range of 700-900 nm (red circles in Fig. S4) is assigned to that of the singlet S_1 decay. We use a bi-exponential function to fit S_1 decay and obtain the normalized dynamics as:

$$A_S(t) = \frac{A_{01}}{A_{01}+A_{02}} e^{\frac{-t}{\tau_1}} + \frac{A_{02}}{A_{01}+A_{02}} e^{\frac{-t}{\tau_2}} = 0.75e^{\frac{-t}{2.5}} + 0.25e^{\frac{-t}{20}} \quad \text{(S1)}$$

where the time unit is in ps and the grey curve in Figure S4 shows the fit.

The bleaching signal at wavelength < 560 nm is a sum of S_0 bleaching in the presence of S_1 and T_1 excitons, and ESA by S_1 and T_1 (individual or in BE). The time dependent bleaching (normalized) is given by:

$$A_B(t) = -\left[A_S(t)(1-\gamma) + 0.5\eta e^{\frac{-t}{\tau_{SF}}} + (\gamma - 0.5\eta)e^{\frac{-t}{\tau_{BE}}} + \eta(1 - e^{\frac{-t}{\tau_{SF}}})\right] \quad \text{(S2)}$$

The time dependent of the ESA for triplet (normalized) is:

$$A_{IA}(t) = \sigma\left[\beta A_S(t)(1-\gamma) + \eta e^{\frac{-t}{\tau_{SF}}} + (2\gamma - \eta)e^{\frac{-t}{\tau_{BE}}} + \eta\left(1 - e^{\frac{-t}{\tau_{SF}}}\right)\right] \quad \text{(S3)}$$

The dynamics for probing wavelength < 560 nm is given by:

$$A(t) = C[A_B(t) + A_{IA}(t)] \tag{S4}$$

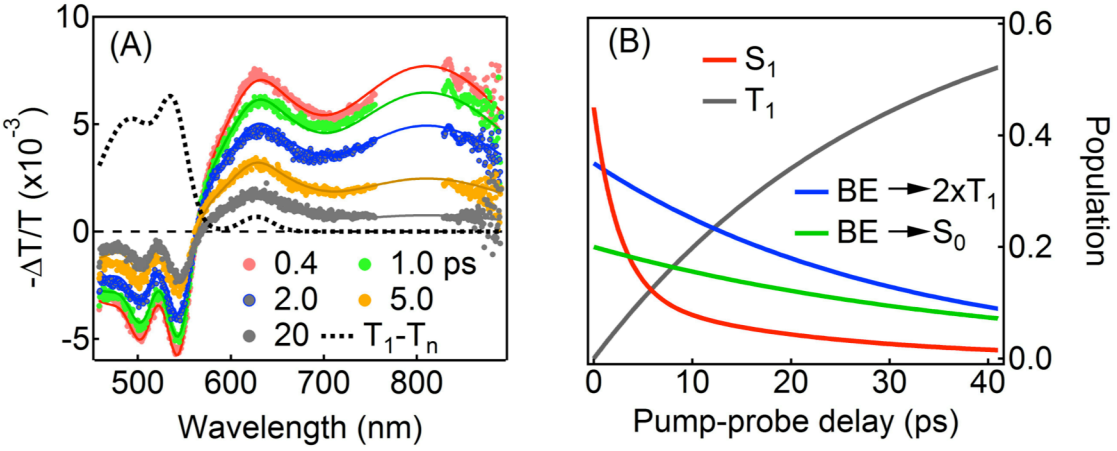

Figure S3. Quantitative analysis of TA spectra from DPDC$_7$ thin film. (A) Experimental TA spectra (dots) at the indicated pump-probe delays with global fits (lines) (red: 0.4 ps; green: 1 ps; blue: 2 ps; orange: 5 ps; grey: 20 ps); Dotted line is ESA of T_1 or BE to higher triplet state (T_n) obtained from the global fits. (B) Populations of singlet S_1 (red), triplet T_1 (grey), multi-exciton (blue & green for the portions converting to triplets or decay to the ground state, respectively).

where C is a fitting constant; γ is the fraction of BE given above; η is singlet fission yield; σ is the ratio of T_1 ESA to S_0 bleaching at a certain wavelength in the presence of a triplet exciton; β is a fraction ESA by singlet S_1, ($\sigma > 0, \beta \geq 0$).

We use a sum of Gaussians to represent each spectral feature and the time dependent spectra is given by

$$S(t,\lambda) = A_B(t)\sum_{i=1}^{3} A_i e^{-\left(\frac{\lambda-\lambda_i}{w_i}\right)^2} + A_{IA}(t)\sum_{i=4}^{6} A_i e^{-\left(\frac{\lambda-\lambda_i}{w_i}\right)^2} + A_S(t)\sum_{i=7}^{8} A_i e^{-\left(\frac{\lambda-\lambda_i}{w_i}\right)^2} \tag{S5}$$

where we use i = 1-3 for S_0 bleaching, with the amplitudes $A_i < 0$; i = 4-6 for ME/T_1 ESA, with $A_i > 0$; i = 7, 8 for singlet ESA, with $A_i > 0$; λ_i is the central wavelength of each Gaussians; w_i is the Gaussian width.

From the fitting, we obtain the following parameters (γ = 0.55; τ_{S1} =2.5 ± 0.5 ps; τ_{BE} = 40 ± 10 ps; τ_{SF} = 30 ± 8 ps) and a singlet fission quantum yield of 70% (number of triplets per absorbed photon). The corresponding kinetic profiles are shown as solid curves in S3-B. Here BE

population consists of two parts: one portion (green) decays back to S_0 via S_2 and the other (blue) separates into two triplets. The fitting result (grey dashed curve in Fig. 4D, main text) accounts for the time profile of GB.

This model provides excellent fits to transient absorption spectra at all pump-probe delays, Fig. S3-A. The ESA for T_1 in Fig. S3 shows that there is a small portion of the T_1 ESA at ~630 nm, which overlaps with the ESA from S_1 and BE at the same wavelength. In this model, the conversion BE into 2xT_1 does not change the ESA spectra since the overall population of the triplet pair is a constant, but the decay of BE to S_0 does show up in the dynamics at 630 nm. Figure S4 shows the dynamic profiles at 630 nm and 765 nm, respectively. The dynamics at 765 nm is purely due to S_1 decays to S_0 (it goes to zero on a long time scale) while that at 630 nm includes residual signal due to ESA from T_1. While the S_1 decay dynamics at 765 nm is described by $A_S(t)$ in equation S_1, the overlapping S_1 and BE decay dynamics at 630 nm can be described by:

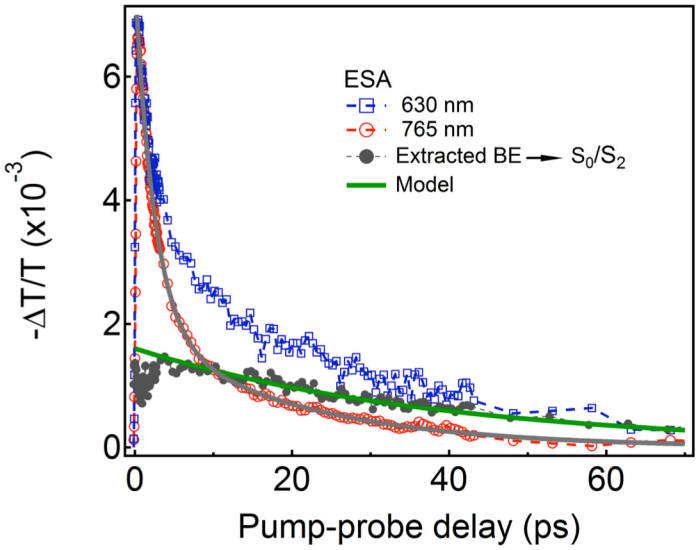

Figure S4. The excited state absorption (ESA) at two different peaks, probing at 630 and 765 nm, black and yellow solid lines are the fits. The black solid circles are the extracted BE→S_0 dynamics, green solid line comes from the above model.

$$A_{S1BE}(t) = aA_S(t) + be^{\frac{-t}{\tau_{BE}}} + C_0 \qquad \text{(S6)}$$

where C_0 is a constant that comes from long lived triplet excitons; τ_{BE} comes from the dynamic fitting using equation S4. From this fit we can extract the BE→S_2/S_0 decay dynamics. The extracted data for BE→S_2/S_0 decay (grey dots) is in excellent agreement with the model.

4. Spectra and dynamics at a long pump-probe delay

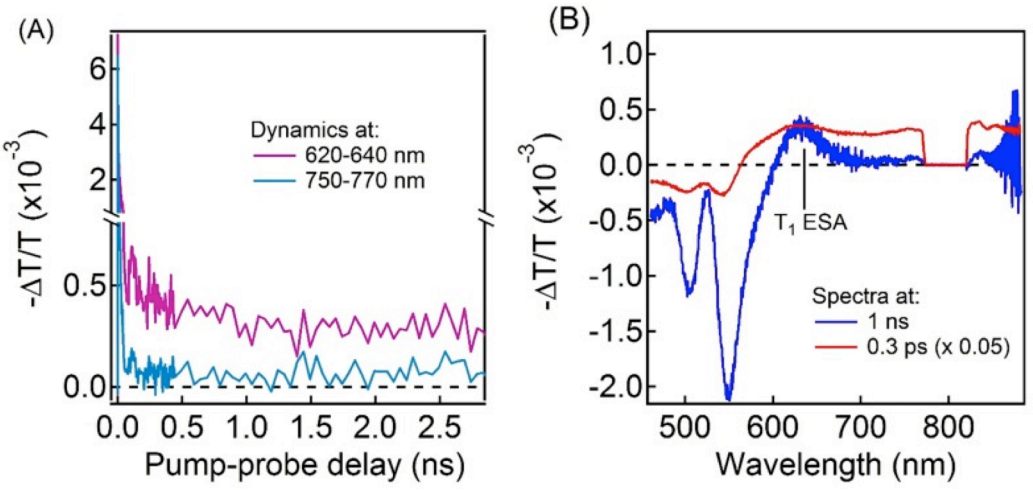

Figure S5. (A) Dynamics averaged from 620 to 640 nm and 750 to 770 nm for $DPDC_7$ in film, pumped at 2.75 eV. (B) Spectra at pump-probe delay of 0.3 ps (scaled by 0.05) and 1ns. There is clear T_1 ESA at 630 nm for a long pump-probe delay spectrum. Note that for spectrum at 1ns the region at the wavelength > 850 nm is noise due to weak probe intensity.

5. Thermal effect exclusion

One might argue that the long lived bleaching single presented in the main text may come from a thermal effect, which caused the modulation in the absorption spectrum of the solid film, as reported for poly(3-hexylthiophene)[4] and acenes.[5,6] We show the absence of this artifact in our measurements.

To describe the relationship of spectral shift and differential intensity (change of the absorption amplitude), we assume that the absorption spectrum is describe by sum of Gaussian functions. The change of amplitude, ΔA, as a function of spectral shift, $\Delta\lambda$, is given by:

$$\Delta A = A_0 e^{-\left(\frac{\lambda-\lambda_i}{w_i}\right)^2} - A_0 e^{-\left(\frac{\lambda-\lambda_i-\Delta\lambda}{w_i}\right)^2} \quad \text{(S7)}$$

In a small shift we can rewrite the eq (S7) as:

$$\Delta A = A_0 e^{-\left(\frac{\lambda-\lambda_i}{w_i}\right)^2} [-\Delta\lambda^2 + 2\Delta\lambda(\lambda - \lambda_i)]$$

In case $\lambda = \lambda_i - \Delta\lambda$

$$\frac{\Delta A}{A_0} = e^{-\left(\frac{\Delta\lambda}{w_i}\right)^2} [-3\Delta\lambda^2] \quad \text{(S8)}$$

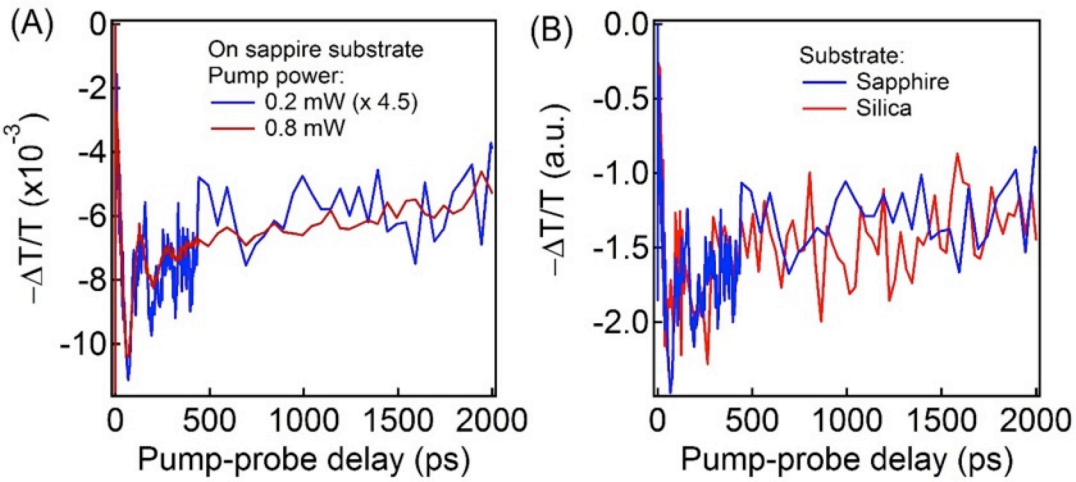

Figure S6. (A) Bleaching dynamics at 555 nm for $DPDC_7$ in film, pumped at 3.54 eV at 0.2 mw (blue, scaled by 4.5) and 0.8 mW (red) showing the same dynamics. (B) Bleaching dynamics at 555 nm for $DPDC_7$ on sapphire (blue) and silica (red) substrates, pumped at 3.54 eV and 0.2 mW.

Clearly that the change of the absorption amplitude is nonlinearly depending on the spectral shift, and so the excitation intensity. Figure S6 (A) shows two time profiles for the bleach signal at 555 nm for a $DPDC_7$ thin film excited at the same photon energy of 3.54 eV, but at different laser powers: 0.2 and 0.8 mW. Within experimental uncertainty, the magnitude of bleaching is proportional to the excitation laser power, but the growth and recovery dynamics are the same. Note that $\Delta A/A_0 \sim -\Delta T/T$. The GB recovery dynamics only depend on excitation photon energy (Fig. 5C in the main text). A thermal effect may be more pronounced in the less crystallinity samples, but we observed the same long lived GB as in the crystalline $DPDC_7$ with a weaker intensity in the less crystallinity $DPDC_9$ and in the amorphous $DPDC_{11}$. In addition, we obtained the same bleaching dynamics with the sample on sapphire and silica substrates which are very different thermal conductivity, figure S6 (B). Thus, we exclude any artifact due to heating of the film.

6. Transient absorption spectra for different number of π-bonds

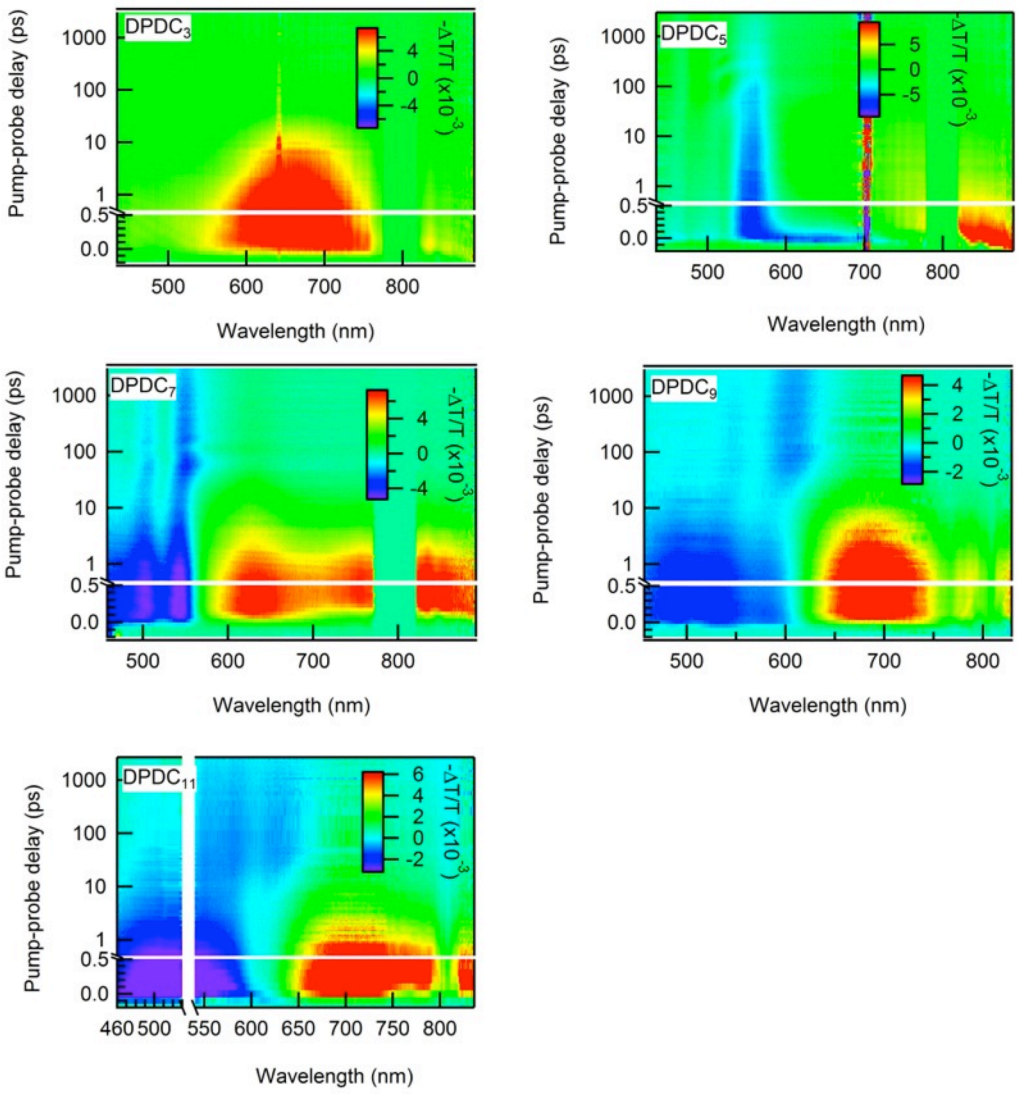

Figure S7. 2D pseudo-color (-ΔT/T) spectra as functions of probe wavelength and pump-probe delay time for $DPDC_n$ in films with different n. The excitation wavelengths are 320 nm (n = 3); 420 nm (n = 5); 450 nm (n = 7); 420 nm (n = 9); and 525 nm (n = 11)

7. Time-dependent density-functional theory (TD-DFT) calculation

Across the series that we studied the energies of both T_1 and S_2 decrease as the number of conjugated π-bonds increase. Consistent with this is the observation that while the energy of the HOMO increases the energy of the LUMO remains roughly constant. The T_1-S_2 splitting also decreases as the number of conjugated double bonds increases. To a first approximation this

splitting is given by 2K, where K is the exchange integral between the two singly-occupied orbitals. As the length of the conjugated chain increases each of the two singly-occupied orbitals that define the excited states extends over a wider area, and it is reasonable that the exchange integral between them is reduced.

Table 1. TD-DFT calculation for different number of π-bonds. Energy is in hartrees (h) unit, except the last two columns are in eV.

Molecule	$E(S_0(h))$	$E(S_2(h))$	$E(T_1(h))$	$E(S_2)$-$E(S_0)$	$E(T_1)$-$E(S_0)$	$E(S_2)$ (eV)	$E(T_1)$ (eV)
DCDP-3	-880.0266	-879.9037	-879.95332	0.1229	0.0733	3.3447	1.9933
DCDP-5	-1034.8548	-1034.7491	-1034.7968	0.1057	0.0580	2.8763	1.5776
DCDP-7	-1189.6724	-1189.5800	-1189.6234	0.0924	0.0490	2.5143	1.3334
DCDP-9	-1344.4993	-1344.4161	-1344.4545	0.0832	0.0448	2.2640	1.2191
DCDP-11	-1499.3210	-1499.2458	-1499.2802	0.0752	0.0408	2.0463	1.1116

8. Crystallinity for $DPDC_n$ films.

We investigate the crystallinity and molecular orientation of $DPDC_n$ films as a function of the number of π-bonds, n, using Grazing Incidence X-ray Diffraction (GIXD). The data, shown in Fig. S8, reveals a trend of crystallinity with the molecular length. The large number of distinct peaks (spots) in the 2-D reciprocal space images ordered along q_r (in the plane: parallel to the substrate) and q_z (out-of-plane: perpendicular to the substrate) for n = 3 indicates that $DPDC_3$ with short chain lengths is highly crystalline and oriented. The textured diffraction rings observed for $DPDC_5$ and $DPDC_7$ also indicate good crystallinity, with smaller population of crystals with a single preferential orientation. Indeed, the degree of crystallinity decreases with increasing chain length so that by $n \geq 9$, the DPDC film is almost amorphous and very weak diffraction peaks are observed.

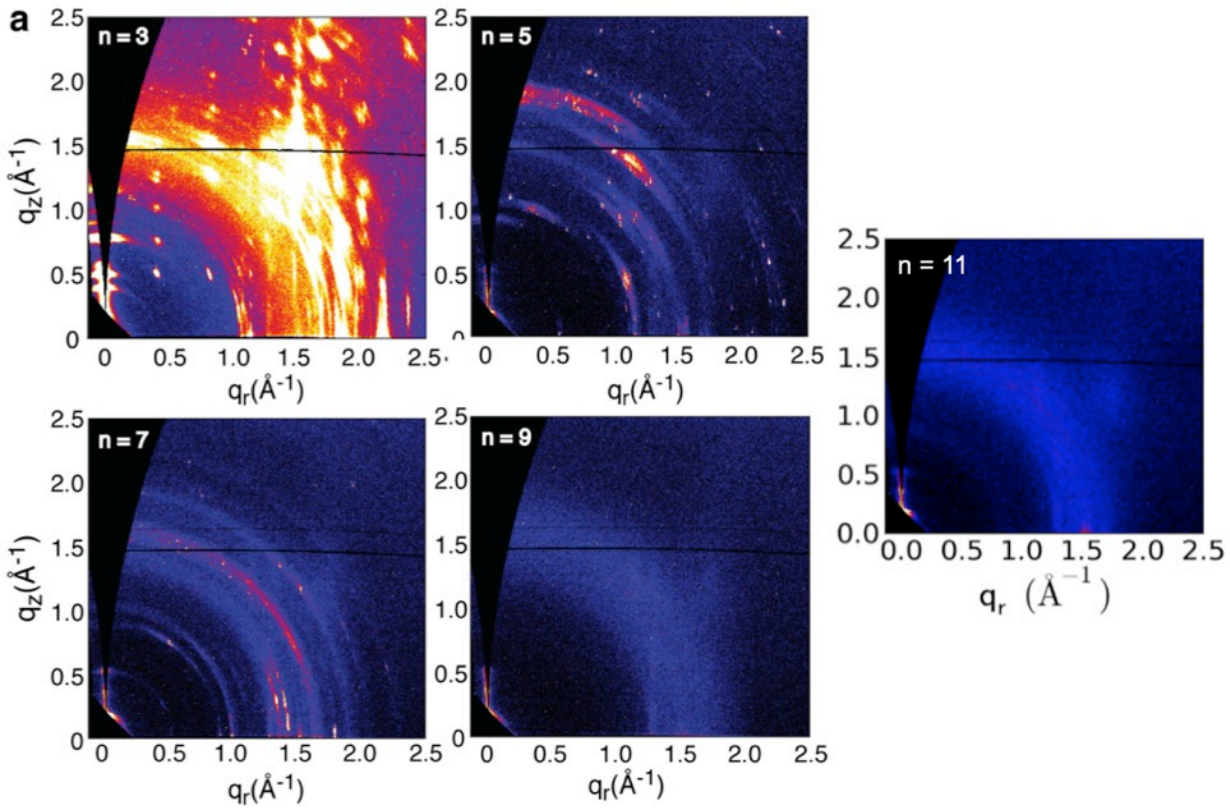

Figure S8. 2-D GIXD patterns, measured at an incident angle of 0.7º, for $DPDC_n$ films as a function of the number of π-bonds along the chain.

9. Picosecond acoustics

The ~100 ps time scale oscillations in the TA spectra (Fig. 5C) are the well-known acoustic waves intrinsic to pulsed laser measurements on thin films.[7,8] The gradient in absorbed energy from the excitation laser pulse creases a strain field and launches an acoustic wave traveling perpendicular to the thin film surfaces, leading to oscillatory changes in optical properties. As expected for the acoustic wave, the time-period of the oscillation depends on film thickness. Fig. S9 shows time profiles of the ground state bleaching signal probed at 555 nm for two $DPDC_7$

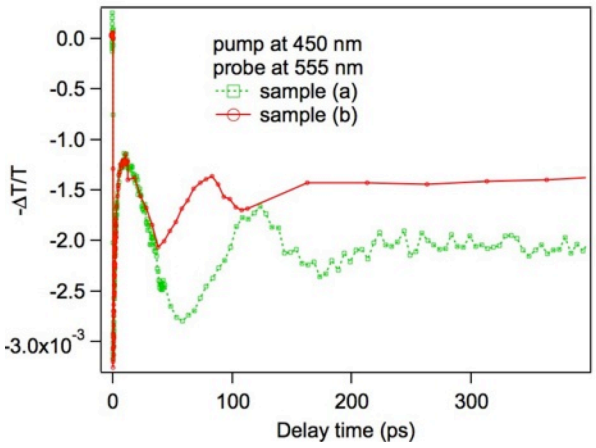

Figure S9. Transient absorption time profiles for two $DPDC_7$ thin film samples pumped at 450 nm and probed at 555 nm (averaged in the range of 550 to 560 nm). Sample (b) is thinner than (a) as seen from optical density.

thin film samples. Here sample (b) is thinner than sample (a) as determined visually from the optical density. The time periods of the oscillation are ~120 ps and ~60 ps in samples (a) and (b), respectively.

10. Chirp correction

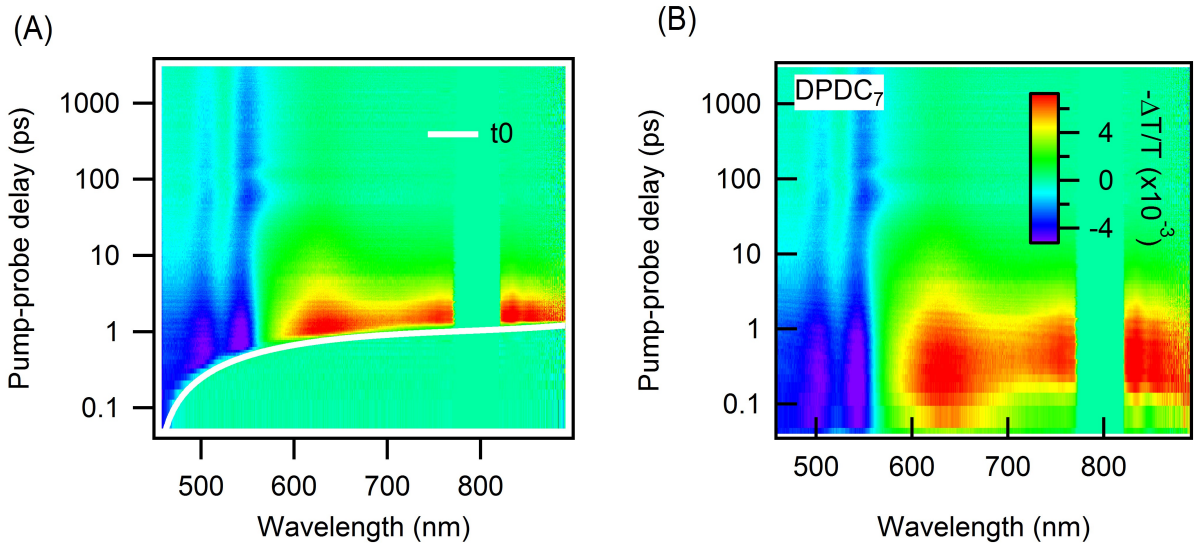

Figure S10. 2D pseudo-color (-ΔT/T) spectra as functions of probe wavelength and pump-probe delay time before (A) and after (B) chirp correction. t0 in (A) is the chirp response as a function of probe wavelength. t0 was obtained from a reference sample with a strong signal in the probe range. Note that the plots are in log scale.

References

1. Gradinaru, C. C. et al. *Proc. Natl. Acad. Sci. U.S.A.* **2001**, 98, 2364–2369.
2. Gradinaru, C. C. Kennis, J. T. M., van Stokkum, I. H. M., Cogdell, R. J. & van Grondelle, R. *Proc. Natl. Acad. Sci. U.S.A.* **2002**, 99, 6017-6022.
3. Antognazza, M. R.; Lüer, L.; Polli, D.; Christensen, R. L.; Schrock, R. R.; Lanzani, G.; Cerullo, G. *Chem. Phys.* **2010**, 373, 115.
4. Albert-Seifried, S.; Friend, R. H. *App. Phys. Lett.* **2011**, 98, 223304
5. Rao, A. *et al. Phys. Rev. B.* **2011**, 84, 195411.
6. Wilson, M. W. B. *et al. J. Am. Chem. Soc.* **2013**, 135, 16680–16688
7. Kanner, G. S., Vardeny, Z. V. & Hess, B. C. P *Phys. Rev. B* **1990**, *42*, 5403-5406.
8. Thomsen, C., Strait, J., Vardeny, Z., Maris, H. J., Tauc, J. & Hauser, J. J. *Phys. Rev. Lett.* **1984**, 53, 989.